Geophysical Journal International

*Geophys. J. Int.* (2011) **185,** 647–652 doi: 10.1111/j.1365-246X.2011.04981.x



# Fe–Ti–O exchange at high temperature and thermal hysteresis

M. Charilaou,[1,2] J. F. Löffler[2] and A. U. Gehring[1]

[1] *Institute of Geophysics, Department of Earth Sciences, ETH Zurich, Sonneggstrasse* 5, 8092 *Zurich, Switzerland. E-mail: michalis.charilaou@mat.ethz.ch*
[2] *Laboratory of Metal Physics and Technology, Department of Materials, ETH Zurich, Wolfgang-Pauli-Strasse* 10, 8093 *Zurich, Switzerland.*

Accepted 2011 February 7. Received 2011 January 31; in original form 2010 September 26

## SUMMARY

In this study, the Fe–Ti–O exchange behaviour between the systems hemo-ilmenite $(y)FeTiO_3$–$(1-y)Fe_2O_3$ and titano-magnetite $(x)Fe_2TiO_4$–$(1-x)Fe_3O_4$ was investigated in the temperature range from 900 to 1400 K in an inert Ar atmosphere. Starting from a mixture of hematite and ilmenite with a fixed mol per cent, heat treatment generates a self-adjusting chemical equilibrium between hemo-ilmenite and titano-magnetite solid solution by means of interdiffusion and $Fe^{3+} \rightarrow Fe^{2+}$ reduction. Structural and magnetic characterization reveals that hemo-ilmenite is stable at all temperatures, whereas titano-magnetite shows increasing Ti-content with increasing treatment temperature. Heating–cooling cycles were performed for a sample to mimic slow cooling and study its effects on the two solid solutions. The magnetic properties of that sample exhibit thermal hysteresis during these cycles, as the Ti departs from titano-magnetite and thus leads to a new chemical equilibrium. The experimental data provide insight into the dynamics of the formation of Fe–Ti–O phases formed under varying conditions in geological systems.

**Key words:** Environmental magnetism; Magnetic mineralogy and petrology; Rock and mineral magnetism; Microstructures; Plasticity, diffusion, and creep.

## 1 INTRODUCTION

The chemical balance in the Fe–Ti–O system between the two solid solution series hemo-ilmenite $(y)$-$FeTiO_3$–$(1-y)Fe_2O_3$ and titano-magnetite $(x)Fe_2TiO_4$–$(1-x)Fe_3O_4$ has been studied for some time (Lindsley 1963; Buddington & Lindsley 1964; Spencer & Lindsley 1981; Hammond & Taylor 1982; Sauerzapf *et al.* 2008). Both series often occur on the Earth, the Moon and very likely on other planets, for example, Mars (Rubin 1997). These solid solution series are characteristics of intrusions and volcanism (McEnroe *et al.* 2001; Lagroix *et al.* 2004). Their chemical composition depends on temperature and oxygen partial pressure, or fugacity $f_{O_2}$ (Lindsley 1963). Thus solid solutions have been used for thermometry to constrain geological processes. This approach was introduced by Lindsley (1963) based on extensive experimental and theoretical data. Recently, the thermo-oxy-barometer was reexamined by Sauerzapf *et al.* (2008), where a combination of data from many works was presented and a newer numerical model derived. All numerical models incorporate both temperature and oxygen fugacity as parameters for the formation of the solid solutions. So far, experimental studies have used the fugacity as a controlled factor, adjusted by means of flowing gas mixtures. However, during the formation of the minerals in natural systems no atmospheric oxygen is present and the fugacity is adjusted by the minerals themselves where oxygen departs or enters the solid state according to temperature and pressure. To simulate an Fe–Ti–O system under conditions of self-adjusting fugacity, an inert atmosphere for the starting condition was chosen. The fugacity is therefore adjusted by temperature-governed redox reactions.

This study presents experimental data on the Fe–Ti–O balance between synthetic hemo-ilmenite and titano-magnetite solid solutions at high temperature ($900 \leq T \leq 1400$ K) and under inert Ar atmosphere, with a fixed overall Ti/Fe ratio. According to temperature and pressure, the hemo-ilmenite phase can convert to titano-magnetite by means of oxygen exchange. In a closed system with an inert atmosphere, oxygen will depart from the solid state of the Fe–Ti–O system by means of $Fe^{3+} \rightarrow Fe^{2+}$ reduction, and thus adjust the fugacity $f_{O_2}$. The generated fugacity corresponds to a specific chemical equilibrium in the system, which is reflected by the composition of the mineral phases or solid solutions. In the self-regulated fugacity approach the equilibrium conditions are probably more complex and therefore traces of additional mineral phases apart from the solid solutions may occur.

To quantify the respective hemo-ilmenite and titano-magnetite compositions, magnetic methods were applied. Both solid solution series exhibit unique magnetic ordering properties, which can be characterized in detail by means of their thermodynamic behaviour. Hemo-ilmenite solid solutions are ferrimagnetic for $y > 0.5$ and antiferromagnetic for $y < 0.5$, and their Curie, or respectively, Néel-temperature $T_C^{HI}$ is a linear function of the composition $y$ (Navarrete *et al.* 2006; Burton *et al.* 2008):

$$T_C^{HI} = 950 - 892\, y. \quad (1)$$

The titano-magnetite series is ferrimagnetic throughout the whole composition range, and its Curie temperature $T_C^{TM}$ is related to the composition $x$ with the empirical expression (Lattard *et al.* 2006):

$$T_C^{TM} = 850 - 580\,x - 150\,x^2. \quad (2)$$

The ordering temperature is an intrinsic property of a magnetic solid phase and is therefore a valuable parameter for determining the composition of solid solutions. This approach can be applied to single solid solutions but also to mixtures of different solid solutions in bulk materials. Among classical experimental methods, ordering temperatures can be determined to high levels of accuracy by means of the thermodynamic *ac* susceptibility $\chi\,(T)$ (Rüdt *et al.* 2004). The *ac* susceptibility $\chi(T)$ is a complex function and consists of an in-phase (real) $\chi'(T)$, and an out-of-phase (imaginary) component $\chi''(T)$: $\chi\,(T) = \chi'(T) + i\,\chi''(T)$. The in-phase component describes the fundamental susceptibility and the out-of-phase the energy dissipations, for example, during magnetic ordering (Prüfer & Ziese 2008). At the onset of magnetic order upon cooling through $T_C$ both in-phase and out-of-phase components exhibit a peak due to fluctuations in the spin structure. The exact $T_C$ can be defined where $\chi''(T)$ becomes non-zero (Rüdt *et al.* 2004), which corresponds to the highest slope of the $\chi'(T)$.

In addition to the Curie or Néel ordering, other transitions have been found in the solid solutions. Synthetic hemo-ilmenite with a composition in the range $0.6 < y < 0.9$ exhibits a spin-glass-like freezing transition (Ishikawa *et al.* 1983, 1985) at $20 < T < 40$ K. In an *ac* susceptibility measurement this transition can be detected by a frequency-dependent drop of the in-phase component with decreasing temperature and a peak in the out-of-phase at the respective freezing temperature $T_f$. Spin-glass properties have also been described in geological samples with $x = 0.8$ (Gehring *et al.* 2007, 2008). In addition, magnetite undergoes a first-order metal-insulator transition at $T_V \approx 120$ K, known as the Verwey transition, which is accompanied by a strong decrease in electron hopping, that is, increase in resistivity upon cooling (Muxworthy & McCelland 2000; Walz 2002). This transition is characterized by a structural change from cubic above $T_V$ to monoclinic below $T_V$, which results in a change of the easy axis of magnetization from (111) to (100) (O'Reilly 1984). In *ac* susceptibility measurements the transition is manifested in a peak in $\chi''(T)$ upon cooling and a subsequent strong fall in $\chi'(T)$ at the transition temperature. The peak in $\chi''(T)$ arises due to energy dissipation during the transition and the reduction of $\chi'(T)$ due to the decrease of the magnetic moment of magnetite. The $T_V$ depends on the stoichiometry of magnetite. Above a certain amount of Ti for Fe substitution ($x > 0.04$) the transition is suppressed (Kakol *et al.* 1992, 1994). Moskowitz *et al.* (1998) reported that the *ac* susceptibility of magnetite containing Ti exhibits a broad decrease with decreasing temperature which becomes less pronounced with increasing Ti content.

In the context of the above magnetic characteristics, it is seen that solid solutions of hemo-ilmenite and titano-magnetite in bulk samples can be magnetically identified and characterized. This allows the quantitative analysis of simultaneously occurring solid solutions with temperature and self-adjusting oxygen fugacity. Such information can provide an insight into geological systems with complex dynamic equilibria.

## 2 EXPERIMENTAL DETAILS

Samples were synthesized from commercial, high-purity (99.99 per cent) $\alpha$-$Fe_2O_3$ and $FeTiO_3$ powders (Alfa Aesar, Germany), with average grain sizes of 44 $\mu$m and 150 $\mu$m, respectively. The powders were weighed to mol percentage for $y = 0.6$, mixed together with a mortar and pestle until a fine mixture was achieved, and then ball-milled in a Planetary Mill at 200 rpm for 2 hr. The fine powder was then pressed in a uniaxial hydraulic press with 80 MPa into six pellets of 10 mm diameter and 2–3 mm thickness. Each pellet was placed on an aluminum oxide $Al_2O_3$ felt substrate and inserted into an individual silica tube, which was then sealed under an inert Ar-atmosphere, with a pressure adjusted to reach 1 atm at the respective sintering temperature. The various tubes with samples of a solid solution series were heated for 24 hr at a temperature between 900 and 1400 K with 100 K intervals. The samples were quenched in water.

The structure of the synthesized solid solutions was studied by means of powder X-ray diffraction in an Xpert PANanlytical diffractometer operating at the Cu $K_\alpha$ line with $\lambda_{K_\alpha} = 1.5405$ Å, in a $2\theta$ range between 20° and 90°, with steps of 0.002°. The pellets were then mechanically polished down to 1 $\mu$m and the local microstructure was examined using a high resolution Hitachi scanning electron microscope (SEM) in high vacuum in field-free mode. The electron backscatter (EBS) detector was used to distinguish between the solid solutions by means of chemical contrast, where the brightness of the element increases with atomic weight: Fe appears lighter than Ti. The chemical composition was semi-quantitatively determined by means of energy dispersive x-ray (EDX) analysis at a beam energy of 20 keV.

Magnetic characterization was performed using a Quantum Design PPMS 6000 with a 9 T superconducting magnet. The *ac* susceptibility of each sample was recorded in a temperature range of 2–300 K, at a frequency of 1.0 kHz, and an external driving field of 5 Oe. The measurement of the high-temperature *ac* susceptibility and the heating–cooling cycles were performed in a Kappabridge KLY-2 in a temperature range of 300–900 K, at 920 Hz and an amplitude of 3.77 Oe. Heating–cooling cycles were performed in the Kappabridge during Ar-flow ranging from 300 to 900 K.

## 3 RESULTS AND DISCUSSION

In the following the six samples prepared at temperatures ranging from 900 to 1400 K are referred to by their sintering temperatures. All samples exhibit XRD peaks that can be assigned to a rhomohedral structure typical for hemo-ilmenite (Brown *et al.* 1993). The fitting of the peaks yields a unit cell volume of $V_{uc} = 311.1(1)$ Å$^3$, which corresponds to a solid solution with composition $y = 0.67(2)$ (Brown *et al.* 1993). This $y$ value is close to the starting composition of $y = 0.6$. For samples 900 through 1200, relatively weak additional peaks were found, which can be attributed to titano-magnetite. The intensity and width of the peaks did not permit the determination of the exact chemical composition of the titano-magnetite. In addition, for samples 1300 and 1400 no defined titano-magnetite peaks could be found, which is probably due to its low concentration in the sample. In the SEM investigations, however, phases from both solid solution series were detected for all samples.

Via SEM the separation of the two phases is possible, because each phase has a different Ti/Fe ratio. This results in a contrast in EBS (see Fig. 1). For samples 900–1100, the two phases consist of isolated micron-sized hemo-ilmenite and nano-sized titano-magnetite particles. For low-temperature sintering ($T < 1100$ K), the hemo-ilmenite phases are inhomogeneous. With increasing sintering temperature, the samples become more compact and massive due to enhanced interdiffusion and increased penetration depth with increasing temperature (Atkinson & Taylor 1985; Sabioni *et al.*

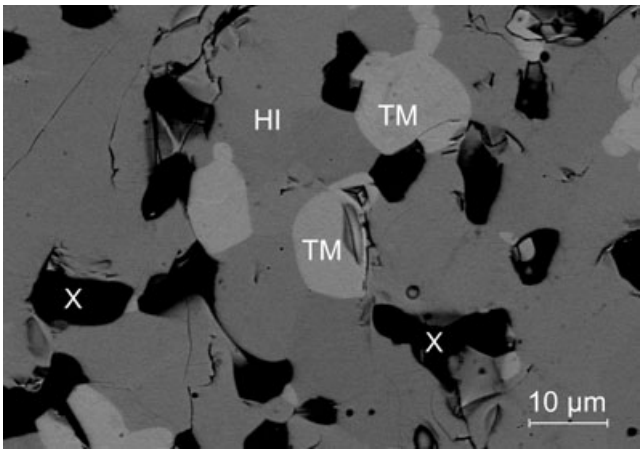


**Figure 1.** Backscattered electron (BSE) image of hemo-ilmenite (dark grey) marked with HI, containing titano-magnetite (light grey) marked with TM, sintered at 1400 K. The black regions such as those marked with X are pores.

2005). The hemo-ilmenite chemistry also becomes more homogeneous and at the same time more Ti is precipitated in the titano-magnetite phase, thus increasing the composition $x$ of the solid solution $(x)Fe_2TiO_4 - (1 - x)Fe_3O_4$. The two solid solutions grow together and the Ti/Fe ratio of titano-magnetite reaches a different equilibrium at each sintering temperature. At the highest, the titano-magnetite grains are embedded inside the hemo-ilmenite host with well-defined grain boundaries, as seen in Fig. 1. The Ti/Fe ratio of the hemo-ilmenite host for sample 1400 was determined by EDX as 0.52(2), which corresponds to a solid solution with $y = 0.68(2)$. This agrees well with the $y$ value of 67(2) deduced from the unit cell volume obtained by XRD. The Ti/Fe ratio in the titano-magnetite was found to be 0.20(3), which corresponds to a solid solution with $x = 0.50(6)$. Because of the small size of the titano-magnetite particles, which is smaller than the electron beam cross-section and the penetration depth at 20 keV, EDX analysis for titano-magnetite formed at $T \leq 1100$ K was not possible.

The measurement of the *ac* susceptibility can overcome these limitations (see Fig. 2). In the high-temperature regime $T > 300$ K, measured using the Kappabridge, all samples exhibit a steep increase in susceptibility upon cooling, which can be attributed to an ordering transition. Sample 900 (a) exhibits an ordering temperature of 835(5) K, which is close to the $T_C = 850$ K of pure magnetite. This suggests a minor Ti content. At the transition a characteristic peak is observed. This peak arises due to the fact that at the onset of magnetic ordering the magnetization $M_S$ increases faster than the magnetic anisotropy $K_1$. Hence, considering that $\chi(T) \propto M_S/\sqrt{K_1}$ (He *et al.* 2000), the so-called Hopkinson peak arises, which is typical for magnetite. The Curie temperature $T_C^{TM}$ decreases with increasing sintering temperature, which confirms the enhanced precipitation of Ti in the solid solution, and reaches a minimum value of $T_C^{TM} = 565(15)$ K for sample 1400. Furthermore, the Hopkinson peak becomes less pronounced and the transition at the Curie point becomes broader with increasing sintering temperature, which results in a larger error in the determination of $T_C^{TM}$. Nevertheless, the Curie temperature can be determined with an accuracy of 5 K for the 900, and 15 K for the 1400 sample. For samples 900 (a) through 1200 (d) the presence of only one feature suggests the dominance of titano-magnetite in the spectrum. The additional peak at about 400 K for samples 1300 and 1400 can be attributed to hemo-ilmenite. A feature at $T = 300$ K which is only observed for sample 1000 (Fig. 2b) cannot be assigned to properties of a Fe–Ti–O

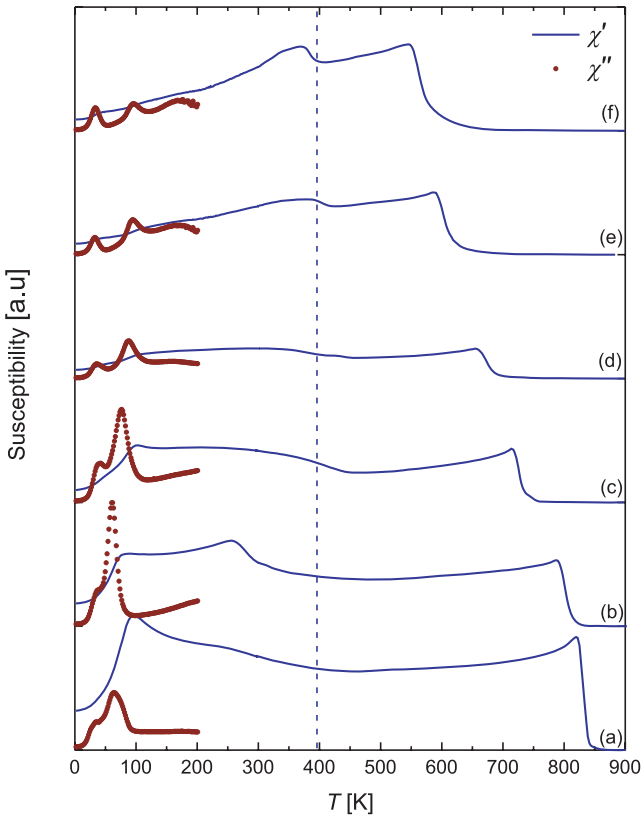


**Figure 2.** Susceptibility of samples 900 (a) through 1400 (f). The solid lines correspond to the in-phase component of the susceptibility $\chi'(T)$, whereas the circles indicate the out-of-phase component $\chi''(T)$. The dashed vertical line near 400 K indicates the position of the $T_C$ of hemo-ilmenite.

solid solution and is probably a sample preparation artefact. Such an artefact may arise from a separate Fe–O phase that is favourable at the temperature range of 1000 K.

The contribution of the hemo-ilmenite phase to the thermodynamic properties of the bulk material upon cooling is indicated by a broad feature in the susceptibility at around 400 K (Fig. 2). At low sintering temperatures (except for 1000), the generally steady increase is most likely due to chemical inhomogeneity. For the samples sintered at high temperature (1300 and 1400), a peak is found at about 400 K, which indicates the ordering temperature of hemo-ilmenite. For sample 1400 the peak is well developed at 390(10) K. This temperature corresponds to a composition of $y = 0.67(2)$ according to eq. (1) and agrees well with the value obtained by XRD and EDX.

For the susceptibility in the low temperature regime $T < 300$ K, both in-phase and out-of-phase components were recorded. For sample 900, the in-phase susceptibility exhibits a pronounced decrease at 100(5) K with decreasing temperature. Since the composition of this sample is close to pure magnetite, this transition is most likely the Verwey transition at $T_V$. The out-of-phase component exhibits a peak at about 64(2) K. Such a peak below the Verwey transition has been reported for magnetite, and was explained as energy dissipation at the point where electron hopping ceases (Kronmüller & Walz 1980; Fischer *et al.* 2008). This transition can be seen in all samples where the decrease in the in-phase component is less pronounced with increasing sintering temperature, and for sintering temperature $T \geq 1200$ K is blurred. In contrast, the peak found in sample 900 in the out-of-phase component is detectable in all

samples and is shifted slightly to higher temperature with higher sintering temperature. Since Ti for Fe substitution suppresses the Verwey transition, as indicated in the in-phase component, the shift of the peak in the out-of-phase component is probably also due to increasing Ti-content.

At $30 \pm 5$ K, a second feature is detected in the out-of-phase susceptibility of all samples. This feature is developed as a shoulder in the samples 900–1000 and as a well-defined peak in samples sintered at higher temperatures. Such a feature is most likely a spin-glass-like freezing transition in hemo-ilmenite (Ishikawa *et al.* 1983, 1985; Gehring *et al.* 2007).

Using eq. (2) the composition $x$ of the titano-magnetite solid solutions sintered at different temperatures is deduced from the $T_C^{TM}$ (Table 1). Sample 900 with $x = 0.03(1)$ is characterized by a nearly pure magnetite, whereas sample 1400 shows the highest Ti for Fe substitution, resulting in $x = 0.42(5)$.

The quantitative data in Table 1 have been used to draw a pseudo-phase diagram of the titano-magnetite solid solution (Fig. 3). In a first approximation, the phase composition has a linear dependence on temperature (Fig. 3). A linear behaviour, however, is rather unrealistic since both, diffusion kinetics and chemical thermodynamics are exponential functions of temperature. A closer examination of the data points agrees with an exponential relation between the temperature and the composition $x$. The course of the data reveals a weak curvature with a flattening point near $x = 0.11(2)$. In the extensive work of Lindsley (1963), where such systems were investigated with various hemo-ilmenite compositions, the miscibility of the titano-magnetite was found to be strongly dependent on the hemo-ilmenite-host composition. Since a curvature with a flattening point at $x = 0.11(2)$ was also observed by Buddington & Lindsley (1964) (Fig. 8) it can be argued that this is an intrinsic titano-magnetite percolation threshold for Ti in magnetite.

**Table 1.** Determination of the chemical composition $x$ of the titano-magnetite phase from its $T_C^{TM}$ for samples sintered at different temperatures $T_{sint}$. The $T_C^{TM}$ was determined at the point of highest slope of $\chi'(T)$.

| $T_{sint}$ [K] | $T_C^{TM}$ [K] | $x$ | Ti/Fe ratio |
|---|---|---|---|
| 900 | 835(5) | 0.03(1) | 0.010(8) |
| 1000 | 800(5) | 0.08(2) | 0.030(8) |
| 1100 | 725(5) | 0.19(3) | 0.07(1) |
| 1200 | 670(10) | 0.28(3) | 0.10(1) |
| 1300 | 605(10) | 0.37(4) | 0.14(2) |
| 1400 | 565(15) | 0.42(5) | 0.16(2) |

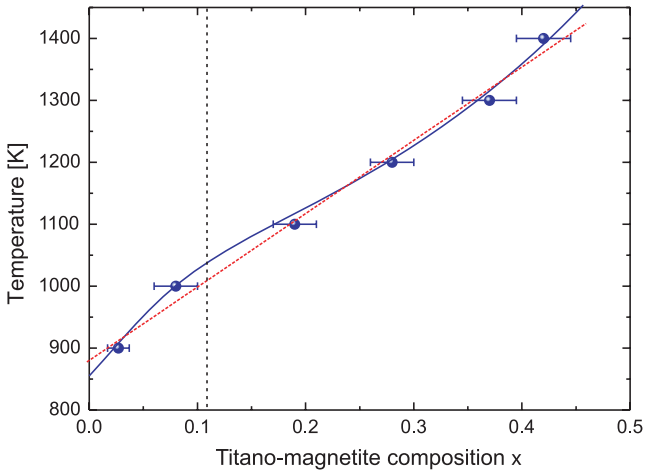


**Figure 3.** Pseudo-phase diagram for the composition $x$ of the titano-magnetite solid solution. The error bars result from the error in the determination of $T_C$. The dashed straight line corresponds to a purely phenomenological linear fit of the data and the solid line represents an alternative exponential fit. The dotted vertical line indicates the position of the percolation threshold.

The data in Fig. 3 can be fitted by a purely phenomenological exponential function in which the hemo-ilmenite composition is also taken into account. The percolation threshold of Ti in magnetite is also considered. The resulting expression is

$$T = \left[855(10) + 150(5)e^{x/\alpha(y)} \tanh(x/0.11)\right] \text{ K}, \quad (3)$$

where $\alpha$ is a function of the hemo-ilmenite composition $y$ and describes the effect of the hemo-ilmenite host on the miscibility of the titano-magnetite. This is done by scaling the titano-magnetite composition in the exponent with a characteristic composition value, which depends on the hemo-ilmenite composition. Sauerzapf *et al.* (2008) studied the dependence of the titano-magnetite miscibility on the hemo-ilmenite composition extensively and found that a hemo-ilmenite composition of $y = 0.65(5)$ corresponds to a titano-magnetite composition of $x = 0.33(2)$. Using $\alpha(0.65) = 0.33$ in eq. (3) results in a curve which agrees well with the measured data (Fig. 3). It should be noted that this expression is valid only in low $f_{O_2}$ atmosphere and within this temperature range.

Having characterized synthetic samples with known thermal histories, one can now expand the scope of these results towards using them as reference for natural systems where the thermal history is unknown. In this case, a key factor in the Fe–Ti–O equilibrium is the cooling rate of the material. Mineral phases formed at a certain temperature are generally in chemical equilibrium. If the material is quenched, as it is often the case during volcanic eruptions, the chemical equilibrium is preserved due to fast cooling. If the mineral phases are cooled slowly, the chemical equilibrium between the solid solutions changes and adopts an equilibrium that corresponds to the temperature in the system. Cooling rates in geological systems are generally slow and decelerate exponentially. Hence, cooling in geological systems cannot be reproduced directly in experiments. Heating–cooling cycles, however, can be used as a straightforward approach to mimic the effect of slow cooling on the solid solutions. When running such a cycle, the solid solutions undergo chemical changes to reach new equilibrium states that correspond to each temperature. The key point in this process is a constant heating–cooling rate which averages fast and slow kinetics at higher and lower temperatures, respectively. With this in mind, heating–cooling cycles of solid solutions starting in a stable state within a defined temperature range provide a direct insight into the mechanics of re-equilibration in the system at the corresponding temperature.

In the following, the results of the re-equilibration experiments of sample 1400 are presented in detail. Fig. 4 shows the susceptibility during the eight heating–cooling cycles. A broad thermal hysteresis is observed during the first cycle. The Curie point $T_C^{TM}$ is shifted to higher values after each run. This suggests rapid departure of Ti from the solid solution, thus increasing the Fe content of the titano-magnetite. Finally, a quasi-equilibrium is reached after the 8th run, with a Curie temperature of $T_C^{TM} = 830(15)$ K, which corresponds to almost pure magnetite. This composition of magnetite in the system is similar to the chemical composition of magnetite in sample 900. This indicates that the Fe–Ti–O system reaches a different equilibrium at each temperature. Since the Curie temperature of the hemo-ilmenite remains stable throughout the cycles, it can be postulated that the chemical composition of this solid solution is stable.

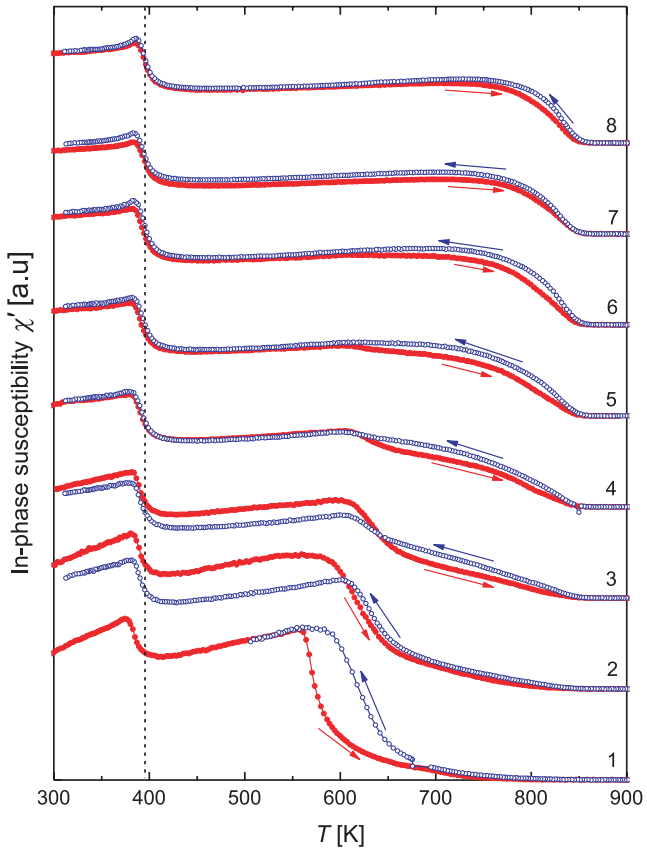


**Figure 4.** Susceptibility of the 1400 sample during eight heating-cooling cycles in the range of 300–900 K.

The low-temperature behaviour of the susceptibility before and after the heating–cooling cycles reveals a change in the out-of-phase susceptibility (Fig. 5). As mentioned above, in the low-temperature range, all samples show two peaks (see Fig. 2). Fig. 5 exhibits the effect of temperature cycling on sample 1400. The peak at about 30 K, attributed to the spin-glass freezing in hemo-ilmenite, is not affected by the temperature cycling. This clearly supports the previous finding that hemo-ilmenite composition is not affected by temperature variations below 900 K. In contrast, the peak at higher

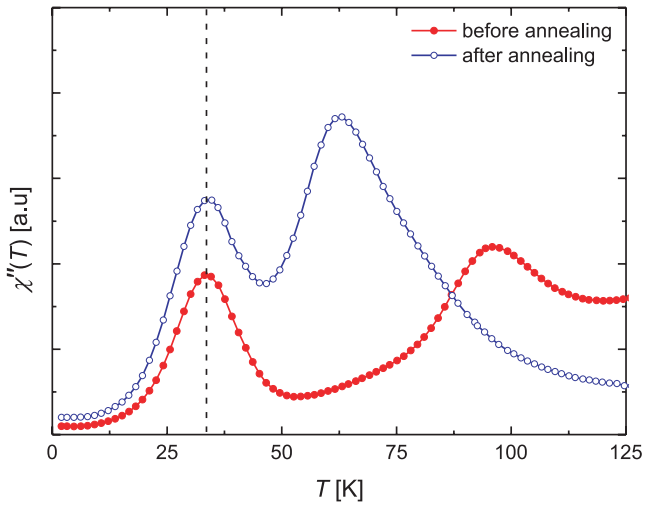


**Figure 5.** Out-of-phase susceptibility $\chi''(T)$ of the 1400 sample before (full circles) and after annealing (open circles).

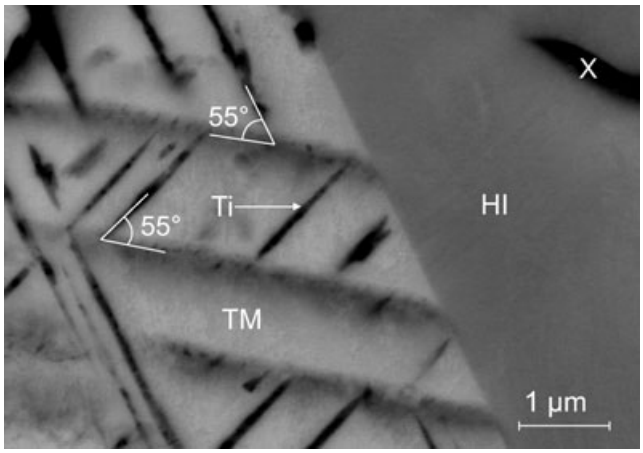


**Figure 6.** Backscattered electron (BSE) image of the sample sintered at 1400 K after it was annealed at 900 K. The light grey area marked with TM is magnetite, and the dark fringes denoted with Ti are $TiO_2$ exsolutions. The dark grey matrix marked with HI is again the hemo-ilmenite solid solution, and the black spot marked with X is a pore.

temperature which is attributed to magnetite reveals a drastic shift to lower temperature. The new position of the peak after annealing at about 65 K coincides with that of sample 900. This shift confirms the decrease of Ti content in the titano-magnetite solid solution. This means that by annealing at a temperature (900 K) lower than the sintering temperature (1400 K), the titano-magnetite phase is re-equilibrated. Similar results have been presented by Lattard *et al.* (2006) and Harrison & Putnis (1996), where the possibility of both exsolution and cation ordering was discussed.

Since hemo-ilmenite remains stable throughout the cycles and the chemical composition of the system is conserved, the re-equilibration of the titano-magnetite has to be balanced by exsolutions. These exsolutions can be seen in the SEM (Fig. 6). As expected, these exsolutions are only associated with magnetite and are Ti-rich. The Ti-rich exsolution fringes as darker areas in the backscatter image follow crystallographic diffusion pathways. The sharp dark fringes rich in $Ti^{4+}$ form an angle of about 55° with lighter blurred exsolution patterns. It is known that for cubic magnetite the angle between the (111) and the (100) planes is 54.74°. It is also known that in magnetite the (111) is the easy and the (100) is the hard direction of diffusion (Augoustithis 1995). Therefore, the two exsolution patterns reflect different diffusion pathways. It can be postulated that the sharp fringes represent fast diffusion along an easy direction, whereas the blurred exsolutions reveal slower kinetics along a hard diffusion axis. Based on the contrast of the dark exsolution fringes and hemo-ilmenite with $y = 0.65$ (Ti/Fe $\approx$ 0.48) it can be assumed that the Ti phase is not a pure Ulvöspinel with a Ti/Fe ratio of 0.5. With this in mind, the dark fringes are formed by titania $TiO_2$, which are diamagnetic and cannot be detected by *ac* susceptibility measurements. The grain boundaries between titano-magnetite and the hemo-ilmenite host remain very sharp, and the hemo-ilmenite host is homogeneous after the annealing cycles. These observations agree well with the stable ordering temperature (see Fig. 4) and indicate that in the low-temperature regime ($T < 900$ K) no oxygen exchange between titano-magnetite and hemo-ilmenite takes place.

## 4 CONCLUSIONS

The thermodynamic behaviour of the magnetic *ac* susceptibility of bulk samples containing hemo-ilmenite and titano-magnetite solid

solution series can be easily used to identify the chemical composition of the two solid solutions.

The chemical equilibrium of hemo-ilmenite and titano-magnetite solid solutions is strongly dependent on temperature. Ti-precipitation in the titano-magnetite phase depends exponentially on temperature, with a flattening point at $x = 0.11(2)$. The latter corresponds to an intrinsic percolation limit of Ti in the titano-magnetite solid solution.

The thermal treatment of the solid solutions in heating–cooling cycles can be used to mimic slow cooling conditions. In these cycles, thermal hysteresis was observed in the magnetic behaviour of the titano-magnetite phase due to Ti-exsolution. In contrast, the hemo-ilmenite phase remains unaffected by the heating–cooling cycles.

Finally, changes in the magnetic properties during the heating–cooling cycles of Fe–Ti–O phases can be a valuable tool for detecting solid solution in bulk samples and in establishing the thermal history of geological systems.

## ACKNOWLEDGMENTS

The authors would like to thank E. Fischer for his assistance in the sample preparation process, J. M. Hickey for various contributions to the project, and Bill Lowrie for the critical review of the manuscript. This work was supported by the Swiss National Science Foundation Grant No. 121844.

## REFERENCES

Atkinson, A. & Taylor, R.I., 1985. Diffusion of $^{55}$Fe in $Fe_2O_3$ Single Crystals, *J. Phys. Chem. Solids,* **46,** 469–475.

Augoustithis, S.S., 1995. *Atlas of the Textural Patterns of Ores Minerals and Metallogenic Processes,* de Gruyter, Berlin.

Brown, N.E., Navrotsky, A., Nord, G.L., Banerjee, S.K., 1993. Hematite-ilmenite ($Fe_2O_3$-$FeTiO_3$) solid solutions: determinations of Fe-Ti order from magnetic properties, *Am. Mineral.,* **78,** 941–951.

Buddington, A.F. & Lindsley, D.H., 1964. Iron-Titanium Oxide Minerals and Synthetic Equivalents, *J. Petrol.,* **5,** 310–357.

Burton, B.P., Robinson, P., McEnroe, S.A., Fabian, K. & Ballaran, T.B., 2008. A low-temperature phase diagram for ilmenite-rich compositions in the system $Fe_2O_3$-$FeTiO_3$, *Am. Mineral.,* **93,** 1260–1272.

Fischer, H., Mastrogiacomo, G., Löffler, J.F., Warthmann, R.J., Weidler, P.G. & Gehring, A.U., 2008. Ferromagnetic resonance and magnetic characteristics of intact magnetosome chains in Magnetospirillum gryphiswaldense, *Earth planet. Sci. Lett.,* **270,** 200–208.

Gehring, A.U., Fischer, H., Schill, E., Granwehr, J. & Luster, J., 2007. The dynamics of magnetic ordering in a natural hemo-ilmenite solid solution, *Geophys. J. Int.,* **169,** 917–925.

Gehring, A.U., Mastrogiacomo, G., Fischer, H., Weidler, P.G., Müller, E. & Luster, J., 2008. Magnetic metastability in natural hemo-ilmenite solid solution (y $\approx$ 0.83), *J. Magn. Magn. Mater.,* **320,** 3307–3312.

Hammond, P.A. & Taylor, L.A., 1982. The ilmenite/titano-magnetite assemblage: kinetics of re-equilibration, *Earth planet. Sci. Lett.,* **61,** 143–150.

Harrison, R.J. & Putnis, A., 1996., Magnetic properties of the magnetite-spinel solid solution: Curie temperatures, magnetic susceptibilities, and cation ordering, *Am. Mineral.,* **81,** 375–384.

He, K., Xu, H., Whang, Z. & Cheng, L., 2000. Hopkinson effect in soft magnetic materials, *J. Mater. Sci. Technol.,* **16,** 145–147.

Ishikawa, Y., Arai, M., Saito, N., Kohgi, M. & Takei, H., 1983. Spin glass properties and magnetic correlation in $FeTiO_3$-$Fe_2O_3$ system, *J. Magn. Magn. Mater.,* **31,** 1381–1383.

Ishikawa, Y., Saito, N., Arai, M., Watanabe, Y. & Takei, H., 1985. A new oxide spin glass system of (1-$x$)$FeTiO_3$-($x$)$Fe_2O_3$. I: magnetic properties, *J. Phys. Soc. Japan,* **54,** 312–325.

Kakol, Z., Sabol, J., Stickler, J. & Honig, J.M., 1992. Effect of low-level titanium(IV) doping on the resistivity of magnetite near the Verwey transition, *Phys. Rev. B,* **46,** 1975–1978.

Kakol, Z., Sabol, J., Stickler, J., Kozkowski, A. & Honig, J.M., 1994. Influence of titanium doping on the magnetocrystalline anisotropy of magnetite, *Phys. Rev. B,* **49,** 12 767–12 772.

Kronmüller, H. & Walz, F., 1980. Magnetic after-effects in $Fe_3O_4$ and vacancy-doped magnetite, *Phil. Mag. B,* **42,** 433–452.

Lagroix, F., Banerjee, S.K. & Jackson, M.J., 2004. Magnetic properties of the Old Crow tephra: identification of a complex iron titanium oxide mineralogy, *J. geophys. Res.,* **109,** B01104, doi:10.1029/2003JB002678.

Lattard, D., Engelmann, R., Kontny, A. & Sauerzapf. U., 2006. Curie temperatures of synthetic titanomagnetites in the Fe-Ti-O system: effects of composition, crystal chemistry, and thermomagnetic methods, *J. geophys. Res.,* **111,** B12S28, doi:10.1029/2006JB004591.

Lindsley, D.H., 1963. *Fe-Ti Oxides in Rocks as Thermometers and Oxygen Barometers*. Vol. 60, Carnegie Institution of Washington Yearbook 62, Washington, D.C.

McEnroe, S.A., Robinson, P. & Panish, P.T., 2001. Aeromagnetic anomalies, magnetic petrology, and rock magnetism of hemo-ilmenite- and magnetite-rich cumulate rocks from the Sokndal Region, South Rogaland, Norway, *Am. Mineral.,* **86,** 1447–1468.

Moskowitz, B.M., Jackson, M. & Kissel, C., 1998. Low-temperature magnetic behavior of titanomagnetites, *Earth planet. Sci. Lett.,* **157,** 141–149.

Muxworthy, A.R. & McClelland, E., 2000. Review of the low-temperature magnetic properties of magnetite from a rock magnetic perspective, *Geophys. J. Int.,* **140,** 101–114.

Navarrete, L., Dou, J., Allen, D.M., Schad, R., Padmini, P., Kale, P. & Pandey, R.K., 2006. Magnetization and Curie Temperature of Ilmenite-Hematite Ceramics, *J. Am. Ceram. Soc.,* **89,** 1601–1604.

O'Reilly, W., 1984. *Rock and Mineral Magnetism,* Blackie, Glasgow.

Prüfer, S. & Ziese, M., 2008. Study of magnetization processes using higher harmonic ac-susceptibility, *Phys. Stat. Sol. (b),* **245,** 1661–1668.

Rubin, A.E., 1997. Mineralogy of meteorite groups, *J. Meteorit. Planet Sci.,* **32,** 231–247.

Rüdt, C., Jensen, P.J., Scherz, A., Lindner, J., Poulopoulos, P. & Baberschke, K., 2004. Higher harmonics of the ac susceptibility: analysis of hysteresis effects in ultrathin ferromagnets, *Phys. Rev. B,* **69,** 014419, doi:10.1103/PhysRevB.69.014419.

Sabioni, A.C.S., Huntz, A.M., Daniel, A.M.J.M. & Macedo, W.A.A., 2005. Measurement of iron self-diffusion in hematite single crystals by secondary ion-mass spectrometry (SIMS) and comparison with cation self-diffusion in corundum-structure oxides, *Phil. Mag.,* **85,** 3643–3658.

Sauerzapf, U., Lattard, D., Burchard, M. & Engelmann, R., 2008. The Titanomagnetite/Ilmenite equilibrium: new experimental data and Thermo-oxybarometric application to the crystallization of basic to intermediate rocks, *J. Petrol.,* **49,** 1161–1185.

Spencer, K. & Lindlsey, D.H., 1981. A solution model for coexisting iron-titanium oxides, *Am. Mineral.,* **66,** 1189–1201.

Walz, F., 2002. The Verwey transition—a topical review. *J. Phys.: Condens. Matter.* **14,** R285, doi:10.1088/0953-8984/14/12/203.